Ecological Informatics 68 (2022) 101555

Contents lists available at ScienceDirect

Ecological Informatics

journal homepage: www.elsevier.com/locate/ecolinf

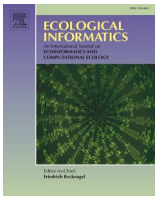

Vegetation recovery and recent degradation in different karst landforms of southwest China over the past two decades using GEE satellite archives

Yuanhuizi He [a,b], Li Wang [a,*], Zheng Niu [a], Biswajit Nath [c]

[a] State Key Laboratory of Remote Sensing Science, Aerospace Information Research Institute, Chinese Academy of Sciences, Beijing 100094, China
[b] University of Chinese Academy of Sciences, Beijing 100049, China
[c] Department of Geography and Environmental Studies, Faculty of Biological Sciences, University of Chittagong, Chittagong 4331, Bangladesh

ARTICLE INFO

Keywords:
Eco-engineering
Vegetation greenness
Southwest karst landforms
Google Earth Engine
Climate change

ABSTRACT

Over the past two decades, eco-engineering has been recognized as an important restoration approach to promote vegetation regrowth and greenness in a widespread rocky desertification land of southwest China. However, it remains unclear of recovery patterns and dominating drivers in different types of karst landforms. Here we use multi-satellite archives based on Google Earth Engine (GEE) to reveal the rapid greening process although encountered severe drought, especially in Karst Peak-Cluster Depression ($+0.0035y^{-1}$) and Karst Trough Valley ($+0.0035y^{-1}$) influenced by subtropical monsoon climate and afforestation endeavor, while degradation happened recently at non-karst areas of west highland in Karst Fault Basin ($-0.0043y^{-1}$ since 2006) and Karst Plateau ($-0.0039y^{-1}$ since 2014) influenced by decreasing rainfall. Afforestation project and sloping land conversion program is found to play crucial part in explaining a large part of the greening trend in Peak-Cluster Depression and Trough Valley but not in other landforms, suggesting that geomorphic heterogeneity should be further considered in restoration implementation and vegetation assessment, in conjunction with climate change and anthropogenic factors. Our study provides a helpful perspective for karst conservation priorities of various rocky desertification region ecosystems.

1. Introduction

Karst is a special landform formed by the long-term dissolution of limestone, coupled with the physical erosion process of water erosion and collapse. The main environmental factors are abundant groundwater, numerous small and medium rivers, limestone with many crevices and voids, as well as erosive surface water. Such environmental factors result in low soil formation rate and high permeability carbonate rocks. Intense soil erosion results in barren soil layer with poor water storage capacity, leading to fragile vegetation resilience and conservation. Land degradation and rock desertification are more likely to occur (Yuan, 1997), which has a dramatic impact on the environment and social economy, such as ecology, soil, carbon-water cycle (Kang et al., 2020; Wang et al., 2017), geological disaster and economic production (Jiang et al., 2014). Karst areas are ecologically fragile areas with frequent vegetation degradation, which increase their sensitivity to environmental changes and human impacts (Wu et al., 2020). Studies on the relationship between vegetation dynamics and climate change are crucial for vegetation protection and restoration of fragile ecosystems (Liu et al., 2018a).

The global karst distribution data released by Karst Scientific Data Center (http://www.karstdata.cn/) shows that the total area of exposed karst landforms in the world is up to 16.72 million square kilometers, covering 12.5% of the global continental (Goldscheider et al., 2020). Literatures up to 2014 shows that the global karst area has reached 22 million square kilometers, accounting for about 15.6% of the world's land surface area and 20% of the total population (Jiang et al., 2014). There are more than 1.88 million square kilometers of karst outcrops and semi-outcrops in China, and the total area of karst areas, mainly in Yunnan-Guizhou and the Qinghai-Tibet Plateau, is 3.44 million square kilometers with the addition of widely distributed limestone rocks buried underground (Wu et al., 2020). Karst regions in southwest China are one of the largest contiguous karst regions in the world, mainly represented by Yunnan, Guizhou, Sichuan, Chongqing, Hunan, Hubei, Guangxi and Guangdong, with a cumulative area of 540,000 km^2 (Wang et al., 2019b). Vegetation there was proved having important carbon sequestration potential for China (Liu et al., 2016a; Song et al., 2016). However, karst areas in southwest China have encountered serious

* Corresponding author.
E-mail address: wangli@radi.ac.cn (L. Wang).

https://doi.org/10.1016/j.ecoinf.2022.101555
Received 8 November 2021; Received in revised form 16 December 2021; Accepted 2 January 2022
Available online 5 January 2022

rocky desertification since around 2000 (Yuan, 1997). Cultivated land expansion and population surge have highlight karst vegetation degradation one of the most important ecological and environmental issues in China (Bai et al., 2013). HengDuan Mountains in southwest China, an important national ecological function zone and ecological barrier of the upper reaches of the Yangtze River, as well as a gathering place of ethnic minorities and poor villages, has witnessed obvious ecological degradation under the influence of human activities and climate change. This has promoted a series of researches on the dynamic evolution of karst vegetation, including the relationship between land use and vegetation degradation (Li et al., 2009; Wang et al., 2004), the evaluation of rocky desertification and the spatiotemporal process of vegetation (Bai et al., 2013; Yue et al., 2012), the attribution analysis of vegetation evolution (Chen et al., 2019; Dai et al., 2017; Jiang et al., 2014; Zhao and Hou, 2019), and the ecological restoration of karst vegetation (Liao et al., 2018).

Since 2000, China has gradually recognized the value of ecosystem services and the sustainable development of fragile ecosystems in karst areas (Li et al., 2021). A series of comprehensive technology has been carried out (Chen et al., 2018; Wang et al., 2019a; Zhang et al., 2020) to address the problems of karst rocky desertification and ecological degradation, and remarkable achievements have been made in ecological protection and restoration (He et al., 2019; Yue et al., 2020; Zhang et al., 2018). Ecological restoration projects have been initiated by Chinese government since the late 1990s to ameliorate degraded environment and alleviate climate stress, including Natural Forest Protection Project (I:2000-2010,II:2011–2020), Green for Grain Project (2002), and the Karst Rocky Desertification Comprehensive Control and Restoration Project(2006–2015). The implementation of national forestry protection activities has increased the coverage of karst vegetation in southern China from 69% to 81% from 1999 to 2017, accounting for about 5% of the global biomass increase (Brandt et al., 2018). Research shows that ecological afforestation projects in karst areas of southwest China improved the ecological environment and carbon sequestration of vegetation, and reduced the sensitivity of karst vegetation ecosystem to climate disturbance (Tong et al., 2018). Forest management has been highly approved to increased vegetation growth and carbon stock in China karst via ecological engineering (Tong et al., 2018; Tong et al., 2020). Ecological engineering has promoted the vegetation restoration rate in China in recent 30 years with a trend of greening, especially in Yunnan, Guangxi and Guizhou provinces (Qiao et al., 2021). its spatial variation still has non-stationary characteristics nevertheless (Tong et al., 2017; Zhang et al., 2017b). Greening trend seems to match with the implementation of ecological conservation projects, while no statistical evidence on a relationship between vegetation greening and eco-engineering exists (Zhang et al., 2021). Due to the particularity of karst ecological landscape (Wang et al., 2014) and the complexity of influencing factors, the phenology (Li et al., 2020) and dynamic changes of vegetation (Tong et al., 2020; Zhou et al., 2017) in karst region still show high spatiotemporal heterogeneity.

Global climate change has strongly enhanced the variability of karst ecosystems in complex climate change (Hou et al., 2015). Although many literatures prove that climate warming promotes the increase of global vegetation coverage, there are also some articles that show that the relationship between karst vegetation and temperature is not significant (Zhao et al., 2020), and even become a limiting factor of vegetation growth in karst areas (Hou et al., 2015). The actual evapotranspiration in karst area is more sensitive to precipitation change under global atmospheric water condition (Liu et al., 2016b). The existence of karst groundwater (Chen et al., 2017) and the process of hydraulic erosion (Dai et al., 2017) also change the soil water holding capacity (Fu et al., 2016) and vegetation available water (VAW) in karst areas (Liu et al., 2018b). Water stress has brought challenges to the utilization of agricultural water resources in karst areas (Wan et al., 2015a) and has become a sensitivity factor affecting the vegetation communities and geomorphic types in karst areas (Zhou et al., 2018). Climate change even weakens the positive effect of vegetation ecological restoration project (Wu et al., 2020), resulting in a more complex relationship between vegetation dynamic change and climate factors. In the face of frequent extreme global climate change, such as drought (Li et al., 2019; Song et al., 2019; Wan et al., 2015a), human interference (Peng et al., 2021; Tong et al., 2016) and land use change (Wang et al., 2020; Yang et al., 2011; Yue et al., 2020). The ecological environment of karst vegetation will be more complicated, and the quantitative study of vegetation dynamic monitoring and climate response will be more meaningful (Zhang et al., 2017a). Under the condition of global climate change, karst vegetation in southwest China plays an important role for China's fragile ecosystem to cope with global change. As a matter of fact, the karst landforms in southwest China are complex and diverse, and the vegetation change and its influencing mechanism under the long-term study scale are still unclear. Therefore, it is necessary to fully understand the current distribution, greening trend and vegetation recovery pattern of typical Karst vegetation in China.

Google Earth Engine (GEE) is a cloud-based planetary geospatial analysis platform, which applies Google's massive computing power to remote sensing research of global change, including vegetable change (Diao et al., 2021; Hansen et al., 2013; Ye et al., 2021; Zhao et al., 2021), land surface water change (Pekel et al., 2016), land use change (Liu et al., 2018c), etc. GEE provides a massive amount of free remote sensing data and an interactive development environment based on Python or JavaScript language, and supports users to calculate worldwide, long time series and multi-source satellite archives. Based on the Google Earth Engine (GEE), a cloud computing platform of, this paper considers typical rocky desertification areas of different karst landforms in southwest China (Karst Peak-Cluster Depression(I) (Zhang et al., 2020), Karst Fault Basin(II) (Li et al., 2020), Karst Plateau(III) (Gao et al., 2012; Xi et al., 2018), Karst Trough Valley(VI) (Xie and Zhao, 2018)) as the study area, and characterize vegetation dynamic change at long-time inter-annual scale. Furthermore, the achievement and its influencing mechanism of vegetation restoration in different karst landforms are discussed, which provides data and theoretical support for ecological restoration of karst rocky desertification region with different landforms.

2. Material and methods

2.1. Study area

Karst Peak-Cluster Depression(I) region is located in Huanjiang (24°44′-25°33′N, 107°51′-108°43′E), north of Guangxi Province. Elevation ranges from 184 m to 1576 m, with high mountains around north and low basin in the south. The region is controlled by an average annual temperature of 19.9 °C in the southern hilly area and 15.7 °C in the northern mountainous area, as well as an average annual rainfall of 1750 mm. Karst peak clusters and depressions are concentrated in the southwest of the region, dominated by dark or brown lime soil developed from carbonate rocks, which is prone to convert to shallow soil layers and large slopes, serious soil erosion and rock exposure. Lithology type of western area is dominated by wide range dolomite, while central karst landform is composed of limestone.

A typical Karst Fault Basin(II) is selected in Luxi (24°10′-24°45′N, 103°30′-104°05′E),eastern Yunnan Province. More than 70% of the 1674km^2 area is covered by limestone-dolomite interbedded layer, with an undulating terrain varies from 902 m to 1840 m and an average altitude of 1840 m. The region is characterized by subtropical monsoon climate with an annual average temperature of 15.2 °C and an annual average rainfall of 979 mm.

Puding (26°26′36″-26°31′42″N, 105°27′49″-105°58′51″E), located in the central part of Guizhou Province as a typical Karst Plateau (III) landform, covers an area of 1091km^2. The topography of the region is relatively high, with an average elevation of 1355 m. The region's northern subtropical monsoon humid climate has formed a mild climate

and abundant rainfall, with an average annual temperature of 15.1 °C and an average annual rainfall of 1396.9 mm. Karst landforms are widely developed with an exposed area of 863.7km^2, accounting for 79.2% of the whole land area.

The Karst Trough Valley (VI) is delineated in the Yinjiang (227°35′-28°28′N, 108°17′-108°48′E) in northern Guizhou, with dolomite as the main karst type. The area presents a sloping landform from southeast to northwest. The highest altitude is 2311 m, the lowest altitude is 458 m, and the average altitude is 910 m. The annual average temperature is 16.8 °C, and the average rainfall is 1113.4 mm (See Fig. 1).

2.2. Multi-source satellite archives on Google Earth Engine and filtered afforestation data

Medium resolution satellite image collection from 2000 to 2020 was download from Google Earth Engine (GEE) platform to describe spatiotemporal variation of vegetation and climate, including (1) MODIS/006/MOD13A2:Global 16-Day Normalized Vegetation Indices (NDVI) at 1 km (Didan, 2015); (2)MODIS/006/MOD11A2: Global Land Surface Temperature(LST) at 1 km (Wan et al., 2015b); (3) MODIS/006/MOD17A2H: Global 8-day Gross Primary Productivity (GPP) at 500 m (Running et al., 2015); (4)MODIS/006/MCD12Q1: MODIS Land Cover Type Yearly Global 500 m, based on Annual International Geosphere-Biosphere Programme (IGBP) classification (Friedl and Sulla-Menashe, 2019); (5) UCSB-CHG/CHIRPS/DAILY: Climate Hazards Group Infrared Precipitation (CHIRPS, Version 2.0 Final), which is a long time series quasi-global rainfall dataset at 0.05° resolution within 50S° to 50 N°. This gridded dataset was produced by satellite imagery and in-situ station data, and was widely applied in trend analysis and seasonal drought monitoring (Funk et al., 2015). In this study, pixel-based quality indicators band for clouds/shadows/land/water mask was applied to the bitmask algorithm for cloud-free images. Annual composites at 1 km for each given year was constructed, including NDVI Maximum Value Composites (NDVI_MVC), LST Mean Value Composite (LST_MVC), GPP Sum Value Composite (GPP_SVC) and CHIRPS Sum Value Composite (CHIRPS _SVC).In addition, 1:500,000 shapefile map of lithology type map acquired from Karst Distribution Map of Southwest China is provided by the Institute of Karst Geology, Chinese Academy of Geological Sciences. Afforestation area was collected from China Forestry Statistical Yearbook (https://data.cnki.net/trade/Yearbook/Single/N2013110040?z=Z010) during 2002 to 2019. Only two data of artificial afforestation and closing hills for reforestation have been compiled and summarized, due to the missing value availability of limited reported materials.

2.3. Sen's slope and Manner-Kendall (M-K) mutation test

Sen's slope and Manner-Kendall (M-K) test have been widely applied in vegetation dynamic and trend analysis (Jiang et al., 2015; Wang et al., 2015). Theil-sen Median method, also known as Sen's slope estimation (Sen, 1968), is a robust trend calculation method of non-parametric statistics. This method has high computational efficiency and is insensitive to measurement error and outlier data, so it is often used in trend analysis of long time series data. The calculation formula is:

$$\text{Slope} = \text{mean}\left(\frac{x_j - x_i}{j - i}\right),\ \forall j > i \tag{1}$$

where x_i and x_j are time series data; i and j represent the year.

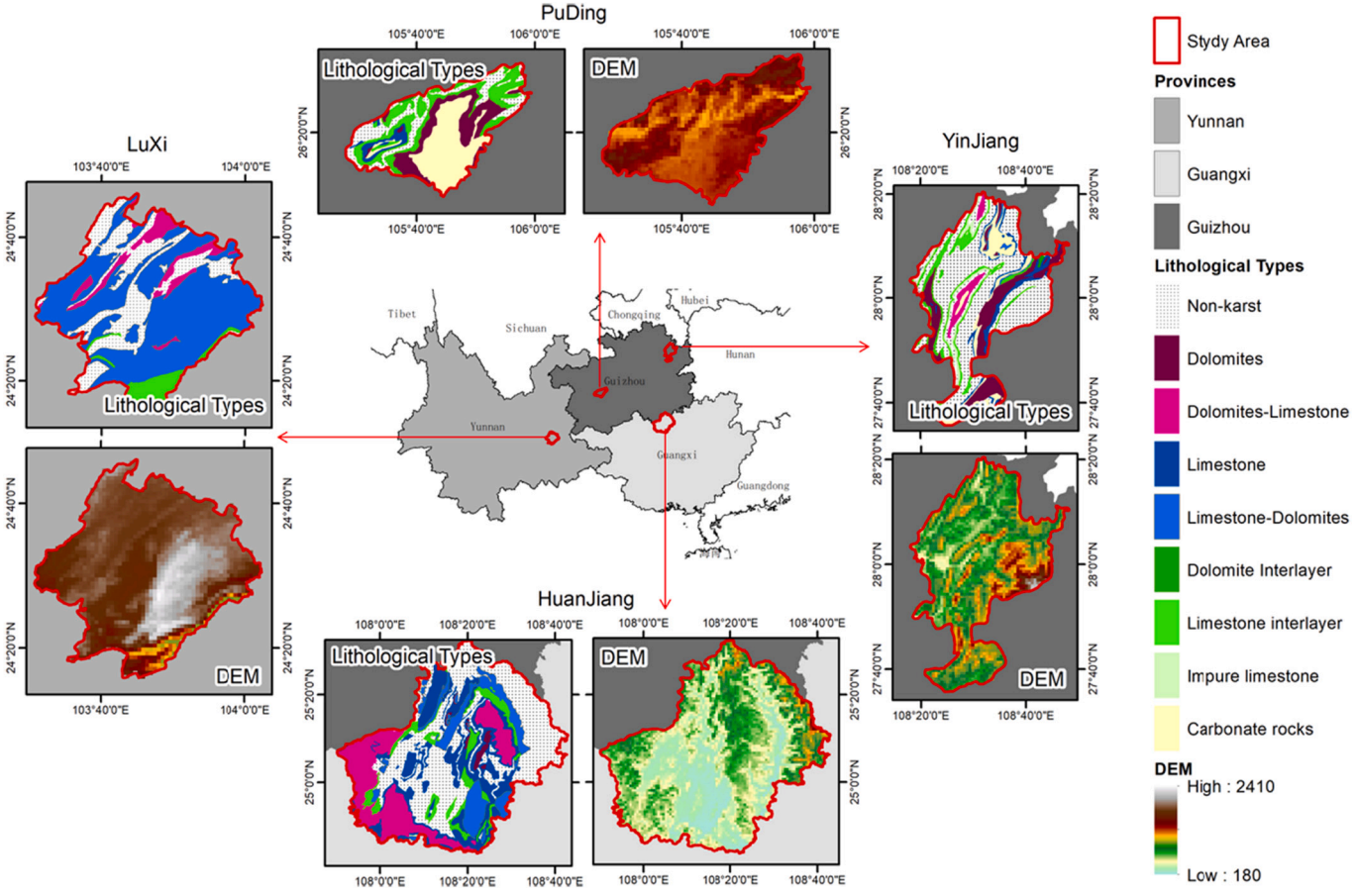

Fig. 1. Geographical location and elevation of the study area with three main lithologic types: **1)** Non-karst type; **2)** Pure karst landscape, including dolomites, dolomite-limestone, limestone, limestone-dolomites; **3)** Impure karst contains dolomites and limestone interlayers, impure limestone and other carbonate rocks.

Manner-Kendall (M-K) (Kendall, 1948; Mann, 1945) is a common mutation detection method that is not only easy to calculate, but also can identify the onset of change point. For time series X with n sample sizes, construct an order column S_k, which is the cumulant whose value at time i is greater than that at time j.

$$S_k = \sum_{i=0}^{k} r_i, (k = 2, 3, \ldots, n) \tag{2}$$

$$r_i = \begin{cases} +1, x_i > x_j \\ 0, else \end{cases}, (j = 1, 2, \ldots, i) \tag{3}$$

Under the assumption of random independence of time series, UF_k is defined as:

$$UF_k = \frac{S_k - E(S_k)}{\sqrt{Var(S_k)}}, (k = 1, 2, \ldots, n) \tag{4}$$

Where $UF_1 = 0$, $E(S_k)$ and $Var(S_k)$ is the mean value and variance of S_k. When $x_1, x_2, \ldots, x_n$ is independent series with the same continuous distribution, it can be calculated by the following formula:

$$E(S_k) = \frac{n(n+1)}{4} \tag{5}$$

$$Var(S_k) = \frac{n(n-1)(2n+5)}{72} \tag{6}$$

Repeat the above process in reverse order $x_n, x_{n-1}, \ldots, x_1$ of time series X, while making $UF_k = -UB_k$, $k = n, n-1, \ldots, 1$, $UB_1 = 0$.

2.4. Pearson correlation between vegetation and climate factors

In order to study the influence of climate conditions on vegetation change in karst areas, the correlation between temperature, precipitation and vegetation index and GPP can be analyzed, which can indicate the relationship between vegetation growth and vegetation change in this region. Pearson correlation coefficient (Benesty et al., 2009) r_{xy} was used to describe the correlation between two variables, and the significance of the correlation coefficient can be tested by *t*-test, which can be divided into significant correlation ($P < 0.05$) and non-significant correlation ($P \geq 0.05$) with 95% confidence. r_{xy} is calculated as follows:

$$r_{xy} = \frac{\sum_{i=1}^{n}(x_i - \overline{x})(y_i - \overline{y})}{\sqrt{\sum_{i=1}^{n}(x_i - \overline{x})^2 \sum_{i=1}^{n}(y_i - \overline{y})^2}} \tag{7}$$

Where n is the image collection length of the study, representing each given year from 2000 to 2020; x_i is an independent variable that changes with time, such as temperature and precipitation. y_i is a dependent variable that changes over time, such as NDVI or GPP. $\overline{x}$ and $\overline{y}$ is the mean value of x and y, respectively.

3. Results

3.1. Climate and vegetation condition among regions

The climate condition of four regions is dominated by the subtropical humid monsoon with mild sunlight and abundant rainfall, whereas there is obvious hydrothermal discrepancy among the regions displayed in

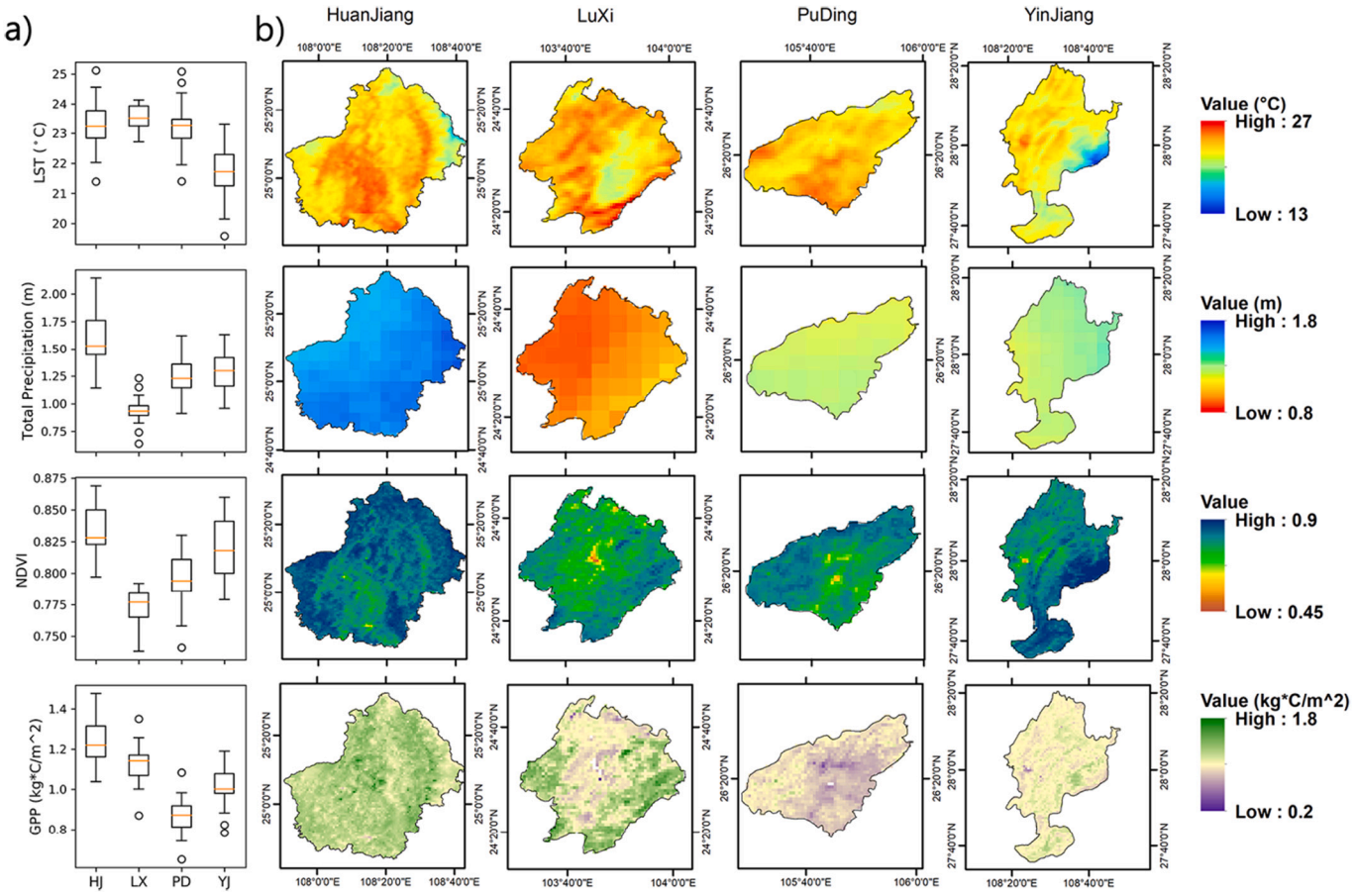

Fig. 2. Spatial hydrothermal and vegetation discrepancy among the regions since 2000.
(a) Mean value of the each region. **(b)** Spatial distribution of climate and vegetation of each region.

Fig. 2(a), mainly affected by tectonic terrace and the rolling hills within the region. Fig. 2(b) shows the monthly mean temperature has fluctuated between 13 °C and 28 °C, with the coolest weather in the southeast hilly area of Yinjiang. Annual precipitation supply level of the region ranges from 800 mm to 1800 mm, with a regional disparity of 1000 mm between Huanjiang and Luxi. Regional mean NDVI has been witnessed staying around at above 0.75 over the last two decades, benefited from our country's afforestation efforts. The vegetation is seen in Fig. 2(a) varying from 0.775 to 0.825 under different water supply conditions hydrothermal level, with the illustration of Huanjiang equipped with excellent warm and humid climate compared to Luxi with less precipitation. The results of GPP distribution in Fig. 2(a) showed that the accumulation of total GPP of each year was 0.8–1.2Pg C/m^2, with the lowest value of 0.2 PgC/ m^2 locally in Puding.

3.2. Vegetation greenness and degeneration along with spatiotemporal climate change

Sen's slope trend analyses show that all of the pixel sequence change with tendency in the last two decades with the large spatial heterogeneity (Fig. 3). Huanjiang were found to be cooling at a maximum average rate of 0.1 °C in depression areas compared to a warmer trend in peak cluster, as well as a wet trend increasing near 20 mm per year in the south area. Greenness and gross primary productivity was observed rising by more than 0.004 and 0.003 Pg C/ m^2 per year. The total precipitation of other three regions was found increasing at a lower rate of 5-15 mm per year. Land surface warming was showed in graben basin in northwest Luxi and carbonate rocks area in Puding, as well as mountain area east of Yinjiang, up to 0.08.°C per year locally. Apparent vegetation degradation have been discovered at non-karst graben basin area in Luxi, with a local pixel NDVI value decreasing at 0.001 per year, while vegetation grow green by more than 0.04 per year and that of GPP by 0.0003 Pg C/ m^2 y^{-1} in the pure limestone-dolomite karst landscape. Vegetation decreasing trend appeared in Puding and Yinjiang in line with the warming area, covered by carbonate rocks and rugged hills.

In addition to temporal tracks of climate and vegetation condition, sudden change point appeared in the time series data have been detected by Manner-Kendall (M-K) mutation test. We divide lithology landform into karst and non-karst categories to compare vegetation and climate level under different geological conditions. Both pure karst landscape and impure karst are considered to be karst areas, with different purity levels. As described in Fig. 4(a), karst regions appeared a slightly cooling tendency ranging from −0.0826 to −0.0158 °C per year, and −0.0885 °C to 0.0084 °C per year for non-karst region that is a little bit lower than karst land in spite of Luxi. In terms of precipitation supply level, Fig. 4(b) characterize a general increase between 18 mm to 20 mm per year for Huanjing, and others that appears slight wetting trend between 7 mm to 11 per year.

As depicted in Fig. 4(c), the vegetation greenness in these typical karst areas in southwest China has been witnessed to grow significantly from 0.78 to 0.86 since 2000, especially in Huanjiang (peak cluster depression region in GuangXi province, slope = 0.0035, R^2 = 0.89) and Yinjiang (trough valley region in GuiZhou province, slope = 0.0035, R^2 = 0.81). Vegetation growth occurred in Luxi in a certain period of time, but a sudden point appeared in 2006 was detected by MK method. NDVI increased by an average of 0.0057 per year (graben basin region in

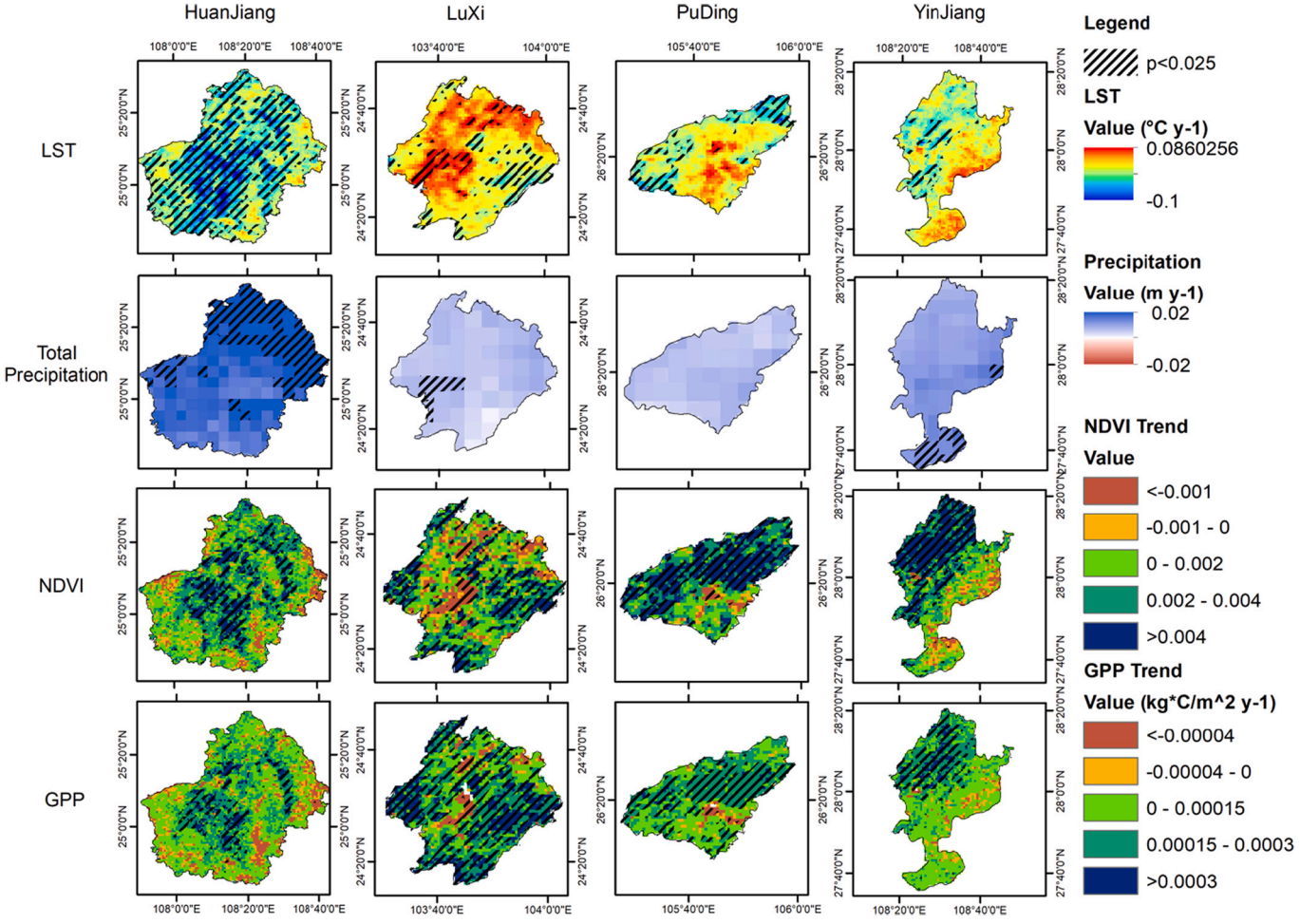

Fig. 3. Spatial tendency of climate and vegetation of four karst regions during 2000–2020.

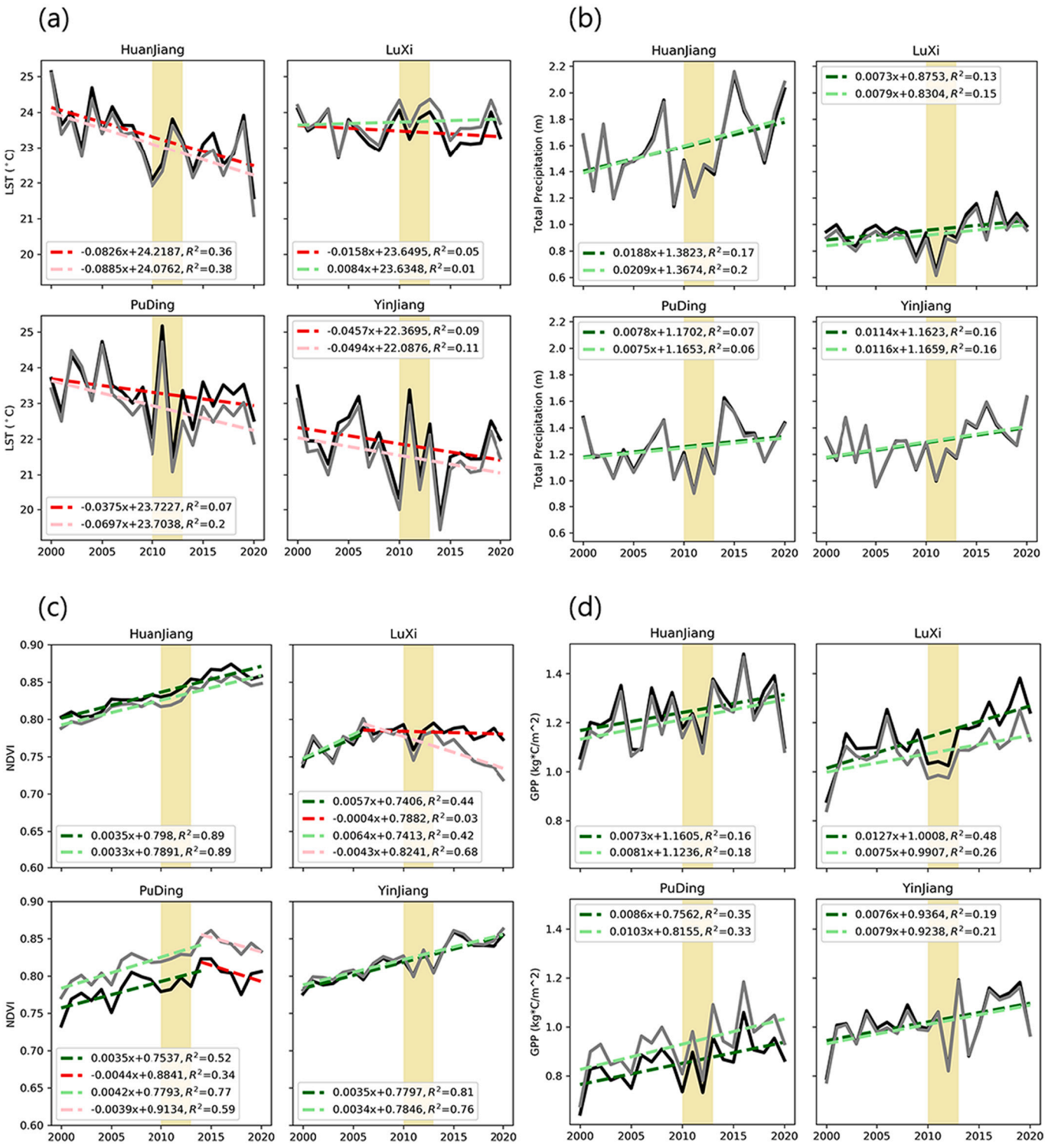

Fig. 4. Temporal tracks of climate and vegetation sequence during 2000–2020. **(a)**LST, **(b)**Total precipitation, **(c)**NDVI, and **(d)**GPP. The black/Gy lines indicate karst/non-karst area, with the trend line colored by green/palegreen or red/pink dash lines, which represent decreasing and increasing trend divided by change point, respectively. The vertical yellow span displays drought event in southwest China during 2010–2012. (For interpretation of the references to colour in this figure legend, the reader is referred to the web version of this article.)

YunNan province, slope = 0.0057, R^2 = 0.44) during 2000–2006, while generally degradation happened during 2006–2020 in the whole watershed level (slope = −0.0004, R^2 = 0.03), especially in non-karst landscapes (slope = −0.0043, R^2 = 0.68). Segmented trend of NDVI was also found in Puding (karst plateau landform in GuiZhou province) during 2000–2014 (slope = 0.0035, R^2 = 0.52) and 2014–2020 (slope = −0.0044, R^2 = 0.34) in karst area, and during 2000–2014 (slope = 0.0042, R^2 = 0.77) and 2014–2020 (slope = −0.0039, R^2 = 0.59) in non-karst area.

GPP has also experienced fluctuating increases since 2000 in Fig. 4 (d), with a total of 88.954PgC/ m^2 captured by the photosynthesis process during the last 20 years in Huanjiang (total GPP = 25.83PgC

/m^2; slope = 0.0073PgC/ m^2 y^{-1} and R^2 = 0.16 for karst; slope = 0.0081PgC/ m^2 y^{-1} and R^2 = 0.18 for non-karst), Luxi (total GPP = 23.607Pg C/m^2; slope = 0.0127PgC/ m^2 y^{-1} and R^2 = 0.48 for karst; slope = 0.0075PgC/ m^2 y^{-1} and R^2 = 0.26 for non-karst), Puding (total GPP = 18.198PgC/m^2; slope = 0.0086PgC/ m^2 y^{-1}, R^2 = 0.35 for karst; slope = 0.0103PgC/ m^2 y^{-1} and R^2 = 0.33 for non-karst;), and Yinjiang (total GPP = 21.319PgC/m^2; slope = 0.0076PgC/ m^2 y^{-1}, R^2 = 0.19 for karst; slope = 0.0079PgC/ m^2 y^{-1}, R^2 = 0.21 for non-karst;).

Apparent fluctuations in temperature and rainfall were shown in Fig. 4(a) and (b) around 2011, which have been confirmed by reported severe drought legacy in southwest China during 2010–2012. Besides, obvious minimum values were observed on vegetation sequences (Fig. 4 (c) and (d)) along with greenness progress during the period of these thirsty years.

3.3. Vegetation recovery along with land cover evolution

Fig. 5 demonstrated land cover change over a period of 20 years, revealing an overall greenness in forest and herbaceous ecosystem in southwest regions of China. HuanJiang was dominated by woody savannas, while its coverage decreased from 65% to 59%, as the evergreen broadleaf forests area increased from 7.6% to 26.7% since 2007, especially in non-karst region from 6.2% to 34.8%. Similar phenomenon happened in YinJiang with mixed forests cover growth from 1.3% to 14.3% and woody savannas increment by 3%. 39.6% of the land surface of LuXi is distributed by cropland in 2004, while only 25.1% remained by the end of 2019, which has been replaced by savannas growing from 56.3% to 70.4%. 22.5% karst cropland in PuDing has been gradually substituted by small-scale cultivation 40–60% with natural tree, shrub, or herbaceous vegetation. All of the surface vegetation cover in four regions has turned lush along with the land cover change, accompanied by vegetation recovery benefiting from either conversion of farmland in LuXi and PuDing, or afforestation in HuanJiang and YinJiang.

3.4. Impacts of climate and effects of ecological restoration activities

According to the correlation coefficients of climate and vegetation sequence depicted in Fig. 6, R value of NDVI-LST is basically negatively in the whole region in line with the vegetation growth and land surface cooling during 2000–2020 seen in Fig. 4. Correlation coefficients of NDVI/GPP- Precipitation are scattered mainly in positive areas, which is in line with the greening trend of vegetation and the precipitation tendency in Fig. 3. There is less significant correlation between GPP and LST although positive R values of GPP-LST were seen in Fig. 6, especially seen in mountainous areas of YinJiang, which can be explained by the fact that vegetation growth is not absolutely subject to temperature and rainfall changes due to the existence of vertical hydrologic structure (Deng et al., 2018). NDVI and GPP are consistent in the overall correlation of the two climate factors, while NDVI shows more significance than GPP, which reflects the discrepancy as proxy in vegetation greenness and productivity for reflecting vegetation growth.

Gross afforestation of 4 typical karst regions was aggregated in Fig. 7-a) annually, comprised by forest plantation in non-forest area and conservation recovery in sparse woods area. The afforestation projects in LuXi and PuDing grew slowly before 2007, with an average of only 693 and 471 ha of newly afforested land during 2004–2007. Fig. 7-b) showed a significant increase forest coverage since 2007 especially in YinJiang County, with an exponentially tendency and a total area up to 85,844 ha. Cumulative afforestation area in Puding is lower than that in Luxi and Huanjiang respectively, while each of the three counties had reached

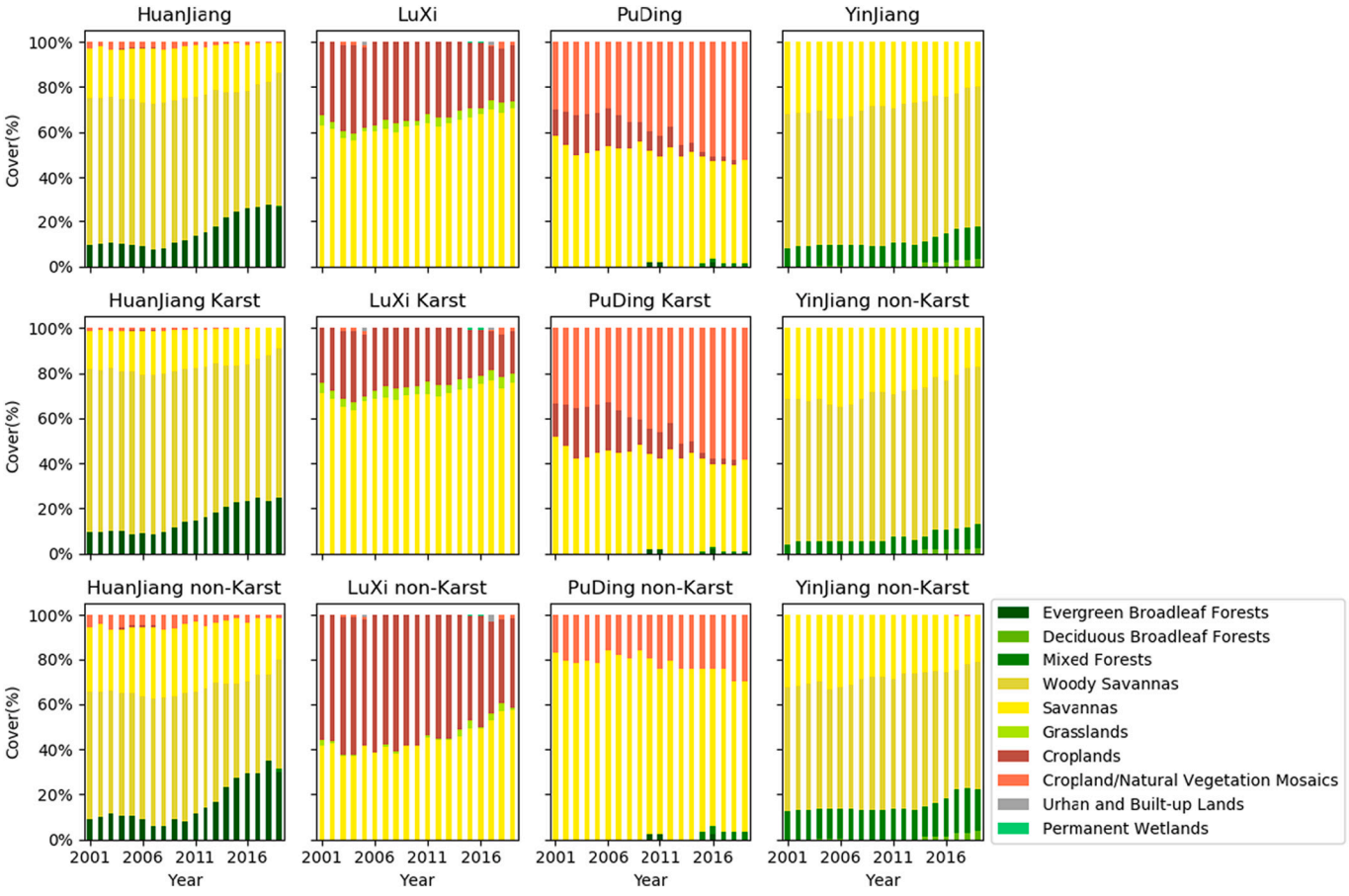

Fig. 5. Vegetation recovery along with the land cover change during 2000–2020.

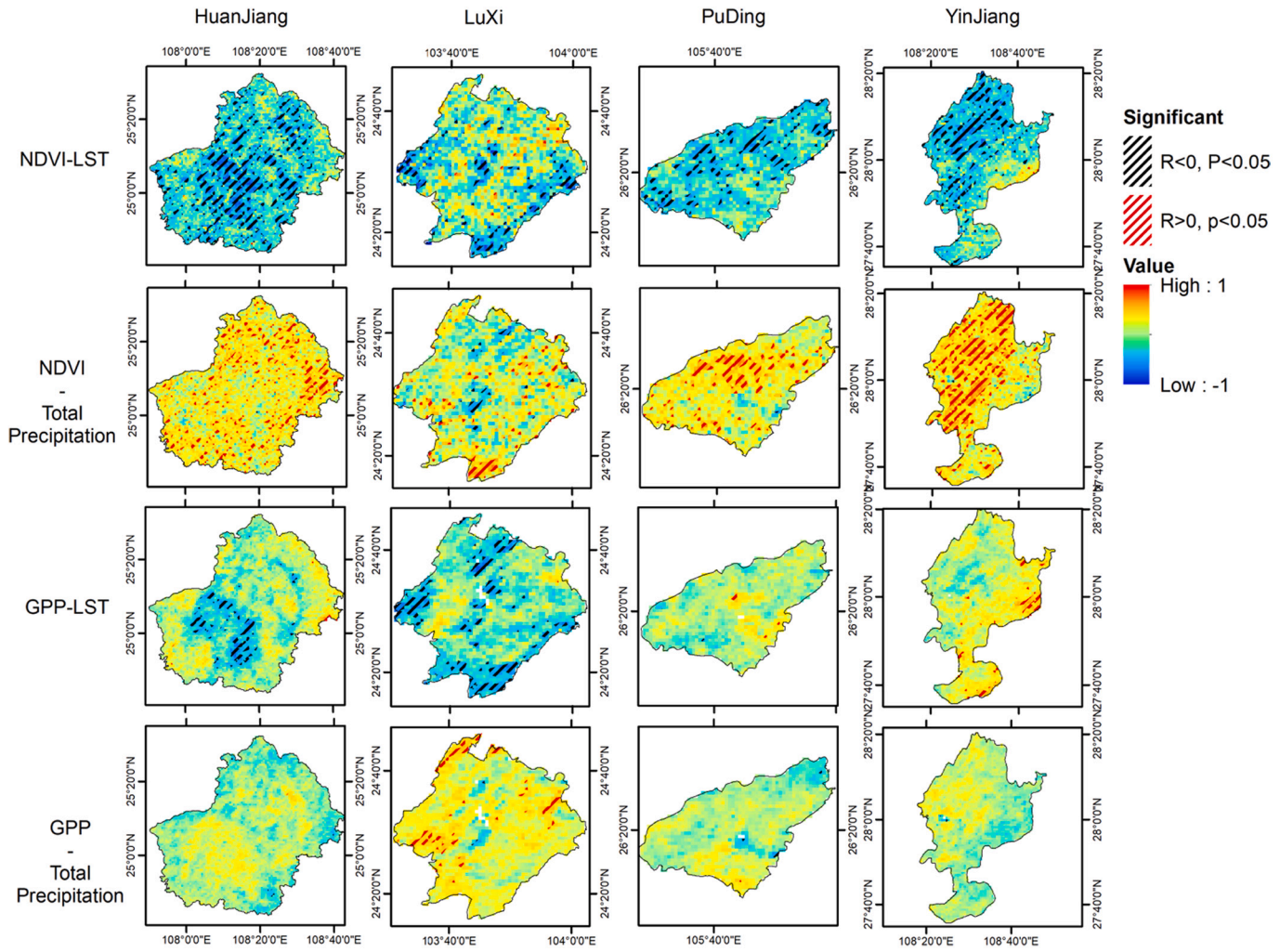

Fig. 6. Spatial correlation coefficient between climate and vegetation variables.

about 50,000 ha by the end of 2019. It is demonstrated in Fig. 7-c) that ecological afforestation implementation seems to match with vegetation growth in karst region, explaining 87% ($p < 0.01$) and 62% ($p < 0.01$) of NDVI dynamics in HuanJiang and Yinjiang, while 85% ($p < 0.01$) and 59% ($p < 0.01$) in that of non-karst area (Fig. 7-d)). There exists no such strongl evidence on a relationship between vegetation greening and eco-engineering in LuXi ($p < 0.1$) and PuDing ($p < 0.1$ in karst area), which is reasonably assumed by the reason that the main recovery and vegetation cover change in Luxi and Puding is farmland returning to woodland and other potential sloping land conversion. The abandon in the area of farmland where crops were originally planted and the increase in sparse shrubs and grasses have probably bring a downward trend in surface NDVI, thus leading to the less significant increase or even decrease in Luxi and Puding. However, it can be seen that the afforestation area does not play a decisive role in the growth of GPP, with R square value lower than 30%. This shows that the increase of afforestation project does not make the same contribution to the improve forest cover and productivity. The raise in forest productivity is affected by other potential complex factors.

4. Discussion

4.1. Focus on the effects of complex variables on vegetation restoration and recovery

Although Fig. 6 shows significant correlation between vegetation cover and hydrothermal variables in local areas, the complicated influence of climate factors cannot be fully understand by limited variable statistics. The karst area in southwest China has a warm climate and abundant rainfall in summer, which not only promotes the growth of vegetation, but also triggers severe erosion power and dissolution conditions for the formation of rocky desertification. Temperature increment has intensified the dissolution process of carbonate substrate, thus limiting soil nutrient accumulation and vegetation growth. In addition, the erosion of rainfall accelerated the chemical reaction between karst matrix and water, resulting in rock desertification. The existence of underground rivers, vertical thermal difference in mountainous area, CO_2 fertilization, as well as other natural factors will increasingly become the key variables in the evolution of karst vegetation.

While the consistency between ecological afforestation and vegetation greening is indicated in this paper, its contribution to vegetation carbon sequestration is not fully discussed. There is no evidence to suggest that afforestation area has played a decisive role on GPP, despite an observed upward trend in Fig. 7. The possible reason is that the ecological engineering records have not been fully collected. Afforestation were used to characterize the intensity of ecological engineering, while other sloping land conversion program and human impacts were not fully considered, including farmland returning to woodland, abandoned land and village migration (Qi et al., 2021), etc. Gap filling and data bank of these projects are of great concern to the research of karst vegetation restoration and recovery.

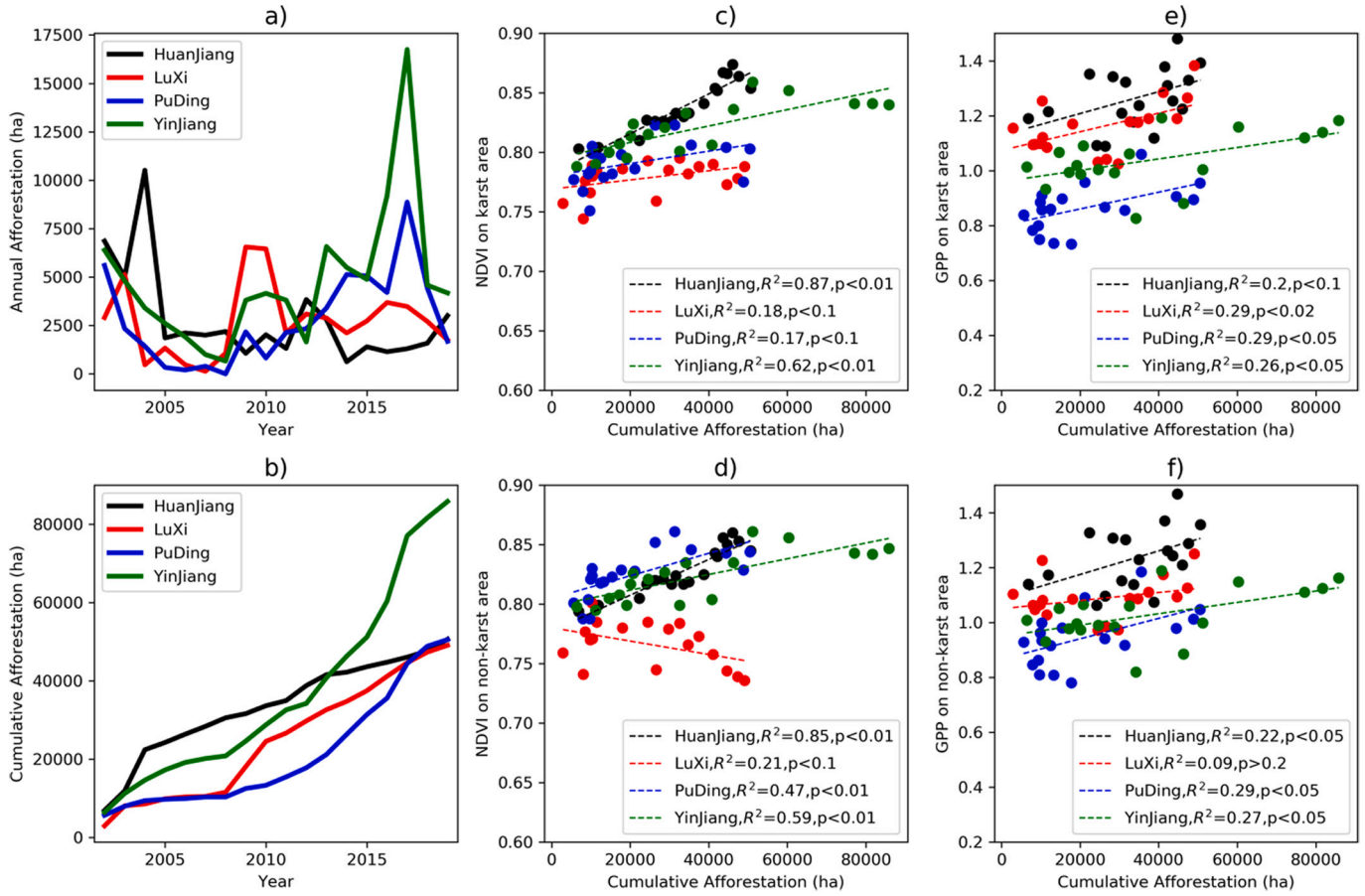

Fig. 7. Afforestation and its impacts on vegetation a) and b) display annual and cumulative afforestation area during 2002–2019. c) and d) show the scatter chart between NDVI and cumulative afforestation area in karst and non-karst region. e) and f) show the scatter chart between GPP and cumulative afforestation area in karst and non-karst region.

4.2. Vegetation condition and dynamics in different geomorphic types

Karst areas in southwest China are typical ecologically fragile areas of serious ecosystem degradation, with complex and diverse geomorphic types, as well as high landscape heterogeneity of ecological environment (Zhang et al., 2021). Typical karst geomorphic types are discussed in this paper, including Karst Peak-Cluster Depression (I), Karst Fault Basin (II), Karst Plateau (III) and Karst Trough Valley (VI). We found that Karst Peak-Cluster Depression (I) (Zhang et al., 2020) and Karst Trough Valley (VI) have the superior climate condition owing to the monsoon climate in the eastern part of Yunnan-Guizhou Plateau, which can be reflected by apparent greenness trend in Fig. 4, no matter the decreasing rainfall and severe drought event (Li et al., 2019). In contrast, Karst Fault Basin (II) and Karst Plateau (III) have more fragile ecological environment and unsteady vegetation evolution, characterized by severe karst leakage and obvious vertical heat difference.

Considering the complexity of karst geological background and the uncertainty in the process of vegetation restoration of rocky desertification, it is of great practical significance to carry out the comprehensive effectiveness evaluation of karst rocky desertification control project. Ecological engineering was the dominant factor in Karst Peak-Cluster Depression (I) and Karst Trough Valleys(VI), explaining 87% and 62% of the positive greening trend, which is consistent with previous studies (Zhang et al., 2021). Specifically, these two types of karst zone were benefited from the superior climate condition (Fig. 2) and rapid afforestation projects (Fig. 7), while Karst Fault Basin (II) and Karst Plateau (III) generally recovered from abandoned land strategies. The discussion of these 4 karst zones and 2 recovery patterns provides important theoretical support for ecological restoration of karst rocky desertification areas with different geomorphic types.

4.3. Limitations and future research directions

Firstly, karst and non-karst regions were considered when discussing vegetation recovery and degradation, while subdivided vegetation cover types have not been fully portrayed. Although annual International Geosphere-Biosphere Programme (IGBP) classification of 500 m in the last two decades was capable of indicating continuous land cover evolution, the savannas in the IGBP classification system does not conform to the real vegetation types in southwest China, and can only reflect the vegetation coverage to a certain extent. Secondly, the spatial resolution of MODIS data set in this paper is still limited in depicting the surface vegetation in southwest China with a specific landscape scale. Coherent high-resolution land classification map and indigenous knowledge are still expected to be adopted in southwest China. Nevertheless, long-term multi-source satellite archives and encapsulated data processing flow provided by GEE platform, still provide irreplaceable scientific tools for long-term and large-scale vegetation dynamic monitoring in the background of global climate change. Thirdly, we highlighted the important role of ecological engineering in improving greenness in four regional landforms, while there are complex variables that have nonlinearly impacts on the process of vegetation growth. In the future, it will be difficult to completely isolate the effects of natural factors and man-made engineering projects on vegetation change. More detailed statistical methods are needed to focus on the coupling relationship between factors and vegetation.

5. Conclusions

In this study, vegetation greenness and degeneration along with spatiotemporal climate change and land cover evolution has been discussed in four typical karst regions, including Karst Peak-Cluster Depression (I), Karst Fault Basin (II), Karst Plateau (III) and Karst Trough Valley (VI). Long-term multi-source satellite archives processing flow based on Google Earth Engine (GEE) and linear statistical methods were adopted to describe vegetation dynamics and its drivers. The results show that heterogeneous vegetation dynamics token place in the last two decades under the impacts of decreasing rainfall and booming eco-engineering. Although ecological afforestation project and sloping land conversion program have explained large part of greening trend in karst areas, rocky desertification still occurs in non-karst areas especially in fault basin of Yunnan and plateau in Guizhou. Research findings remind us paying close attention to the coupling drivers from climate change and human activities in prominent rocky desertification regions, while affirming vegetation greenness and ecological achievement.

Credit authorship contribution statement

Yuanhuizi He: Conceptualization, Methodology, Software, Writing - original draft. Wang Li: Writing - review & editing, Supervision, Project administration, Funding acquisition. Zheng Niu: Project administration, Funding acquisition. Biswajit Nath: Project administration, Funding acquisition.

Declaration of Competing Interest

The authors declare that they have no known competing financial interests or personal relationships that could have appeared to influence the work reported in this paper.

Acknowledgements

This work was supported by the National Natural Science Foundation of China [grant numbers 41871347]; the Strategic Priority Research Program of the Chinese Academy of Sciences [grant number XDA19030404]. We thank NASA LP DAAC at the USGS EROS Center for providing MODIS NDVI, LST, GPP and Land Cover products. We thank UCSB/CHG for providing CHIRPS Daily precipitation products. We thank Google Earth Engine platform for providing massive satellite image processing algorithm and computing power. Institute of Karst Geology, CAS is thanked for providing 1:500,000 shapefile map of lithology type map acquired from Karst Distribution Map of Southwest China.

References

Bai, X., Wang, S., Xiong, K., 2013. Assessing spatial-temporal evolution processes of karst rocky desertification land: Indications for restoration strategies *Land Degrad.* Develop. 24, 47–56.

Benesty, J., Chen, J., Huang, Y., Cohen, I., 2009. Pearson correlation coefficient. Springer.

Brandt, M., Yue, Y., Wigneron, J.P., Tong, X., Tian, F., Jepsen, M.R., Xiao, X., Verger, A., Mialon, A., Al-Yaari, A., Wang, K., Fensholt, R., 2018. Satellite-observed major greening and biomass increase in South China karst during recent decade. Earth's Future 6, 1017–1028.

Chen, Z., Auler, A.S., Bakalowicz, M., Drew, D., Griger, F., Hartmann, J., Jiang, G., Moosdorf, N., Richts, A., Stevanovic, Z., Veni, G., Goldscheider, N., 2017. The World Karst Aquifer Mapping project: concept, mapping procedure and map of Europe. Hydrogeol. J. 25, 771–785.

Chen, H., Yue, Y., Wang, K., 2018. Comprehensive control on rocky desertification in karst regions of southwestern China:achivements, problems, and countermeasures. Carsologica Sinica 37, 37–42.

Chen, F., Wang, S., Bai, X., Liu, F., Zhou, D., Tian, Y., Luo, G., Li, Q., Wu, L., Zheng, C., Xiao, J., Qian, Q., Cao, Y., Li, H., Wang, M., Yang, Y., 2019. Assessing spatial-temporal evolution processes and driving forces of karst rocky desertification. Geocarto International 1–19.

Dai, Q., Peng, X., Yang, Z., Zhao, L., 2017. Runoff and erosion processes on bare slopes in the Karst Rocky Desertification Area. CATENA 152, 218–226.

Deng, Y., Wang, S., Bai, X., Tian, Y., Wu, L., Xiao, J., Chen, F., Qian, Q., 2018. Relationship among land surface temperature and LUCC, NDVI in typical karst area. Sci. Rep. 8, 641.

Diao, C., Liu, Y., Zhao, L., Zhuo, G., Zhang, Y., 2021. Regional-scale vegetation-climate interactions on the Qinghai-Tibet Plateau. Ecol. Inform. 65, 101413.

Didan, K., 2015. In: Daac, N.E.L.P. (Ed.), MOD13A2 MODIS/Terra Vegetation Indices 16-Day L3 Global 1km SIN Grid V006.

Friedl, M., Sulla-Menashe, D., 2019. In: Daac, N.E.L.P. (Ed.), MCD12Q1 MODIS/Terra+ Aqua Land Cover Type Yearly L3 Global 500m SIN Grid V006.

Fu, T., Chen, H., Wang, K., 2016. Structure and water storage capacity of a small karst aquifer based on stream discharge in southwest China. J. Hydrol. 534, 50–62.

Funk, C., Peterson, P., Landsfeld, M., Pedreros, D., Verdin, J., Shukla, S., Husak, G., Rowland, J., Harrison, L., Hoell, A., Michaelsen, J., 2015. The climate hazards infrared precipitation with stations—a new environmental record for monitoring extremes. Sci Data 2, 150066.

Gao, J., Li, S., Zhao, Z., Cai, Y., 2012. Investigating spatial variation in the relationships between NDVI and environmental factors at multi-scales: a case study of Guizhou Karst Plateau, China. Int. J. Remote Sens. 33, 2112–2129.

Goldscheider, N., Chen, Z., Auler, A.S., Bakalowicz, M., Broda, S., Drew, D., Hartmann, J., Jiang, G., Moosdorf, N., Stevanovic, Z., 2020. Global distribution of carbonate rocks and karst water resources. Hydrogeol. J. 28, 1661–1677.

Hansen, M.C., Potapov, P.V., Moore, R., Hancher, M., Turubanova, S.A., Tyukavina, A., Thau, D., Stehman, S.V., Goetz, S.J., Loveland, T.R., 2013. High-resolution global maps of 21st-century forest cover change. Science *342*, 850–853.

He, X., Wang, L., Ke, B., Yue, Y., Wang, K., Cao, J., Xiong, K., 2019. Progress on ecological conservation and restoration for China Karst. Acta Ecol. Sin. 39, 6577–6585.

Hou, W., Gao, J., Wu, S., Dai, E., 2015. Interannual Variations in Growing-Season NDVI and Its Correlation with Climate Variables in the Southwestern Karst Region of China. Remote Sens. 7, 11105–11124.

Jiang, Z., Lian, Y., Qin, X., 2014. Rocky desertification in Southwest China: Impacts, causes, and restoration. Earth Sci. Rev. 132, 1–12.

Jiang, W., Yuan, L., Wang, W., Cao, R., Zhang, Y., Shen, W., 2015. Spatio-temporal analysis of vegetation variation in the Yellow River Basin. Ecol. Indic. 51, 117–126.

Kang, Z., Chen, J., Yuan, D., He, S., Li, Y., Chang, Y., Deng, Y., Chen, Y., Liu, Y., Jiang, G., Wang, X., Zhang, Q., 2020. Promotion function of forest vegetation on the water & carbon coupling cycle in karst critical zone: Insights from karst groundwater systems in south China. J. Hydrol. 590, 125246.

Kendall, M.G., 1948. Rank correlation methods.

Li, Y., Shao, J., Yang, H., Bai, X., 2009. The relations between land use and karst rocky desertification in a typical karst area, China. Environ. Geol. 57, 621–627.

Li, X., Li, Y., Chen, A., Gao, M., Slette, I.J., Piao, S., 2019. The impact of the 2009/2010 drought on vegetation growth and terrestrial carbon balance in Southwest China. Agric. For. Meteorol. 269, 239–248.

Li, D., Wu, X., Zhang, J., Yu, Y., 2020. Vegatation Phenology Change and Response to Climate Change in the Karst Faulted Basin of Southwest China. Res. Soil and Water Conserv. 27, 168–173.

Li, S., Liu, C., Chen, J., Wang, S., 2021. Karst ecosystem and environment: Characteristics, evolution processes, and sustainable development. Agric. Ecosyst. Environ. 306, 107173.

Liao, C., Yue, Y., Wang, K., Fensholt, R., Tong, X., Brandt, M., 2018. Ecological restoration enhances ecosystem health in the karst regions of southwest China. Ecol. Indic. 90, 416–425.

Liu, C., Liu, Y., Guo, K., Wang, S., Liu, H., Zhao, H., Qiao, X., Hou, D., Li, S., 2016a. Aboveground carbon stock, allocation and sequestration potential during vegetation recovery in the karst region of southwestern China: A case study at a watershed scale. Agric. Ecosyst. Environ. 235, 91–100.

Liu, M., Xu, X., Wang, D., Sun, A.Y., Wang, K., 2016b. Karst catchments exhibited higher degradation stress from climate change than the non-karst catchments in southwest China: An ecohydrological perspective. J. Hydrol. 535, 173–180.

Liu, H., Zhang, M., Lin, Z., Xu, X., 2018a. Spatial heterogeneity of the relationship between vegetation dynamics and climate change and their driving forces at multiple time scales in Southwest China. Agric. For. Meteorol. 256-257, 10–21.

Liu, M., Xu, X., Sun, A.Y., Luo, W., Wang, K., 2018b. Why do karst catchments exhibit higher sensitivity to climate change? Evidence from a modified Budyko model. Adv. Water Resour. 122, 238–250.

Liu, X., Hu, G., Chen, Y., Li, X., Xu, X., Li, S., Pei, F., Wang, S., 2018c. High-resolution multi-temporal mapping of global urban land using Landsat images based on the Google Earth Engine Platform. Remote Sens. Environ. 209, 227–239.

Mann, H.B., 1945. Nonparametric tests against trend. Journal of the econometric society, Econometrica, pp. 245–259.

Pekel, J.-F., Cottam, A., Gorelick, N., Belward, A.S., 2016. High-resolution mapping of global surface water and its long-term changes. Nature 540, 418–422.

Peng, J., Jiang, H., Liu, Q., Green, S.M., Quine, T.A., Liu, H., Qiu, S., Liu, Y., Meersmans, J., 2021. Human activity vs. climate change: Distinguishing dominant drivers on LAI dynamics in karst region of southwest China. Sci. Total Environ. 769, 144297.

Qi, X., Qian, L., Yue, Y., Liao, C., Lu, Z., Xuemei, Z., Wang, K.-L., Zhang, C., Zhang, M.-Y., Xiong, Y., 2021. Rural–Urban Migration and Conservation Drive the Ecosystem Services Improvement in China Karst: A Case Study of HuanJiang County, Guangxi. Remote Sens. 13, 566.

Qiao, Y., Jiang, Y., Zhang, C., 2021. Contribution of karst ecological restoration engineering to vegetation greening in southwest China during recent decade. Ecol. Indic. 121, 107081.

Running, S., Mu, Q., Zhao, M., 2015. In: Daac, N.E.L.P. (Ed.), MOD17A2H MODIS/Terra Gross Primary Productivity 8-Day L4 Global 500m SIN Grid V006.

Sen, P.K., 1968. Estimates of the regression coefficient based on Kendall's tau. J. Am. Stat. Assoc. 63, 1379–1389.
Song, X., Gao, Y., Wen, X., Guo, D., Yu, G., He, N., Zhang, J., 2016. Carbon sequestration potential and its eco-service function in the karst area, China. J. Geogr. Sci. 71, 1926–1938.
Song, L., Li, Y., Ren, Y., Wu, X., Guo, B., Tang, X., Shi, W., Ma, M., Han, X., Zhao, L., 2019. Divergent vegetation responses to extreme spring and summer droughts in Southwestern China. Agric. For. Meteorol. 279, 107703.
Tong, X., Wang, K., Brandt, M., Yue, Y., Liao, C., Fensholt, R., 2016. Assessing future vegetation trends and restoration prospects in the karst regions of southwest China. Remote Sens. 8, 357.
Tong, X., Wang, K., Yue, Y., Brandt, M., Liu, B., Zhang, C., Liao, C., Fensholt, R., 2017. Quantifying the effectiveness of ecological restoration projects on long-term vegetation dynamics in the karst regions of Southwest China. Int. J. Appl. Earth Obs. Geoinf. 54, 105–113.
Tong, X., Brandt, M., Yue, Y., Horion, S., Wang, K., Keersmaecker, W.D., Tian, F., Schurgers, G., Xiao, X., Luo, Y., Chen, C., Myneni, R., Shi, Z., Chen, H., Fensholt, R., 2018. Increased vegetation growth and carbon stock in China karst via ecological engineering. Nat. Sustain. 1, 44–50.
Tong, X., Brandt, M., Yue, Y., Ciais, P., Jepsen, M., Penuelas, J., Wigneron, J.-P., Xiao, X., Song, X.-P., Horion, S., Rasmussen, K., Saatchi, S., Fan, L., Wang, K.-L., Zhang, B., Chen, Z., Wang, Y., Li, X., Fensholt, R., 2020. Forest management in southern China generates short term extensive carbon sequestration. Nat. Commun. 11, 129.
Wan, L., Zhou, J., Guo, H., Liu, Y., 2015a. Trend of water resource amount, drought frequency, and agricultural exposure to water stresses in the karst regions of South China. Nat. Hazards 80.
Wan, Z., Hook, S., Hulley, G., 2015b. MOD11A2 MODIS/Terra Land Surface Temperature/Emissivity 8-Day L3 Global 1km SIN Grid V006 (In. NASA EOSDIS Land Processes DAAC).
Wang, S., Liu, Q., Zhang, D., 2004. Karst rocky desertification in southwestern China: geomorphology, landuse, impact and rehabilitation. Land Degrad. Dev. 15, 115–121.
Wang, M., Wang, X., Liang, Z., Wei, X., Li, H., 2014. Landscape pattern analysis on change of fractional vegetation cover between karst and no-karst areas: a case study in Hechi District , Guangxi Zhuang Autonomous Region. Acta Ecol. Sin. 34, 3435–3443.
Wang, H., Chen, A., Wang, Q., He, B., 2015. Drought dynamics and impacts on vegetation in China from 1982 to 2011. Ecol. Eng. 75, 303–307.
Wang, S., Liu, Z., Jian, N., Yan, J., Liu, X., 2017. A Review of Research Progress and Future Prospective of Carbon Cycle in Karst Area of South China. Earth and Environ. *45*, 2–9.
Wang, K., Yue, Y., Chen, H., Wu, X., Xiao, J., Qi, X., Zhang, W., Du, H., 2019a. The comprehensive treatment of karst rocky desertification and its regional restoration effects. Acta Ecol. Sin. 39, 7432–7440.
Wang, K., Zhang, C., Chen, H., Yue, Y., Zhang, W., Zhang, M., Qi, X., Fu, Z., 2019b. Karst landscapes of China: patterns, ecosystem processes and services. Landsc. Ecol. 34, 2743–2763.
Wang, Y., Luo, W., Zeng, G., Peng, H., Cheng, A., Zhang, L., Cai, X., Chen, J., Lyu, Y., Yang, H., Wang, S., 2020. Characteristics of carbon, water, and energy fluxes on abandoned farmland revealed by critical zone observation in the karst region of southwest China. Agric. Ecosyst. Environ. 292, 106821.
Wu, L., Wang, S., Bai, X., Tian, Y., Luo, G., Wang, J., Li, Q., Chen, F., Deng, Y., Yang, Y., Hu, Z., 2020. Climate change weakens the positive effect of human activities on karst vegetation productivity restoration in southern China. Ecol. Indic. 115, 106392.
Xi, H., Wang, S., Bai, X., Tang, H., Wu, L., Chen, F., Xiao, J., Wang, M., Li, H., Cai, Y., Chen, H., Ran, C., Luo, X., 2018. Spatio-temporal characteristics of rocky desertification in typical Karst areas of Southwest China: A case study of Puding County , Guizhou Province. Acta Ecol. Sin. 38, 8919–8933.
Xie, R., Zhao, C., 2018. Spatio-temporal Differentiation of Ecological Environment Vulnerability in Karst Trough Region Based on Grid Scale. J. Yangtze River Sci. Res. Institute 35, 48–53.
Yang, Q., Wang, K., Zhang, C., Yue, Y., Tian, R., 2011. Spatio-temporal evolution of rocky desertification and its driving forces in karst areas of Northwestern Guangxi, China. Environ. Earth Sci. 64, 383–393.
Ye, L., Liu, M., Liu, X., Zhu, L., 2021. Developing a new disturbance index for tracking gradual change of forest ecosystems in the hilly red soil region of southern China using dense Landsat time series. Ecol. Inform. 61, 101221.
Yuan, D., 1997. Rock desertification in the subtropical karst of south China. Z. Geomorphol. Suppl. 108, 81–90.
Yue, Y., Wang, K., Zhang, B., Jiao, Q., Liu, B., Zhang, M., 2012. Remote sensing of fractional cover of vegetation and exposed bedrock for karst rocky desertification assessment. Procedia Environ. Sci. 13, 847–853.
Yue, Y., Liao, C., Tong, X., Wu, Z., Fensholt, R., Prishchepov, A., Jepsen, M., Wang, K.-L., Brandt, M., 2020. Large scale reforestation of farmlands on sloping hills in South China karst. Landsc. Ecol. 35.
Zhang, C., Qi, X., Wang, K., Zhang, M., Yue, Y., 2017a. The application of geospatial techniques in monitoring karst vegetation recovery in southwest China: A review. Progress Phys. Geograph.: Earth and Environ. 41, 450–477.
Zhang, X., Wang, K., Yue, Y., Tong, X., Liao, C., Zhang, M., Jiang, Y., 2017b. Factors impacting on vegetation dynamics and spatial non-stationary relationships in karst regions of southwest China. Acta Ecol. Sin. 37, 4008–4018.
Zhang, M., Wang, K., Liu, H., Zhang, C., Yue, Y., Qi, X., 2018. Effect of ecological engineering projects on ecosystem services in a karst region: A case study of northwest Guangxi, China. J. Clean. Prod. 183, 831–842.
Zhang, X., Qi, X., Yue, Y., Wang, K., Zhang, X., Liu, D., 2020. Natural regionalization for rocky desertification treatment in karst peak-cluster depression regions. Acta Ecol. Sin. 40, 5490–5501.
Zhang, X., Yue, Y., Tong, X., Wang, K., Qi, X., Deng, C., Brandt, M., 2021. Eco-engineering controls vegetation trends in southwest China karst. Sci. Total Environ. 770, 145160.
Zhao, L., Hou, R., 2019. Human causes of soil loss in rural karst environments: a case study of Guizhou, China. Sci. Rep. 9, 3225.
Zhao, S., Pereira, P., Wu, X., Zhou, J., Cao, J., Zhang, W., 2020. Global karst vegetation regime and its response to climate change and human activities. Ecol. Indic. 113, 106208.
Zhao, Y., Feng, Q., Lu, A., 2021. Spatiotemporal variation in vegetation coverage and its driving factors in the Guanzhong Basin, NW China. Ecol. Inform. 64, 101371.
Zhou, J., Ma, M., Xiao, Q., Wen, J., 2017. Vegetation Dynamics and Its Relationship with Climate Factors in Southwestern China. Remote Sens. Technol. and Appl. 32, 966–972.
Zhou, Q., Luo, Y., Zhou, X., Cai, M., Zhao, C., 2018. Response of vegetation to water balance conditions at different time scales across the karst area of southwestern China—A remote sensing approach. Sci. Total Environ. 645, 460–470.